Desalination and Water Treatment
www.deswater.com

doi: 10.5004/dwt.2018.22373

121 (2018) 104–110
July

Research on co-combustion characteristics and kinetics of sewage sludge and rice husk

Anna Liang[a,†], Yiqie Dong[a,†], Teng Wang[a], Yixin Li[a], Yi Han[a], Haobo Hou[a,b], Min Zhou[a,b,*]

[a]*School of Resource and Environmental Sciences, Wuhan University, Wuhan, China, Tel. +86 13871283321; emails: zhoumin@whu.edu.cn (M. Zhou), anna_whu@163.com (A. Liang), dyq_whu@163.com (Y. Dong), 835473515@qq.com (T, Wang), 2437753561@qq.com (Y, Li), yihan@whu.edu.cn (Y. Han), hhb-bhh@163.com (H. Hou)*
[b]*Hubei Environmental Remediation Material Engineering Technology Research Center, Wuhan*

Received 25 February 2018; Accepted 12 April 2018

ABSTRACT

According to the characteristics of high moisture content and low calorific value of sludge, an innovative co-combustion method of sewage sludge and rice husk was proposed. The method provided a theoretical basis for the resource utilization of sewage sludge. Through thermal analysis technology, the changes of thermogravimetric and derivative thermogravimetric at different temperatures with various ratios of mixed combustion materials were investigated. Then, the corresponding dynamic model was established to analyze the dynamic mechanism of the co-combustion material. The following conclusions were obtained: First, the combustion of mixed fuel when the amount of sludge is less than 30% is beneficial. Therefore, the use of sewage sludge as fuel to combustion is possible. Moreover, the kinetic mechanism of the combustion reaction can be divided into four processes, that is, one-dimensional diffusion, chemical reaction, one-dimensional diffusion, and three-dimensional diffusion.

Keywords: Sewage sludge; Rice husk; Combustion kinetics; Resource utilization; Combustion characteristics

1. Introduction

With the increasing attention focused on sewage treatment in China, the urban sewage treatment rate also increases. For this reason, the amount of municipal sludge increases sharply every year. According to the results of relevant investigation, the average daily wet sludge production of China reached 61,000 t, and most of the sludge treatment was landfill. A disadvantage of landfill is that it occupies a large area of land and produces serious secondary environmental pollution [1]. Rice husk, as a by-product of agricultural production, has a large annual output. Most of the rice husk is treated by incineration directly with a low utilization rate [2].

Scholars have determined that the harmful components in dewatered sludge can be reduced by incineration. By contrast, the combustible components of rice husk account for more than 70%, with the calorific value of 12.5–14.6 MJ/kg, which is approximately half of that of coal. The co-combustion of sludge and rice husk can deal with the problems of the increasing amount of sludge and the agricultural waste disposal of rice husk. The heat generated by the co-combustion of sludge and rice husk can meet the demand of heat and power generation of industrial boilers and relieve the energy pressure [3]. However, research on the co-combustion of sewage sludge and rice husk is scarce in the country and abroad.

In this study, the thermal and gravimetric changes of mixed material are investigated by thermal analysis of

* Corresponding author.

† The authors contributed equally to this paper.

Presented at the 3rd International Conference on Recent Advancements in Chemical, Environmental and Energy Engineering, 15–16 February, Chennai, India, 2018.

the co-combustion process of sludge and rice husk. The thermochemical characteristics of the sludge and rice husk mixture with different ratios are investigated [4]. The kinetic model of the combustion reaction is established by combining the kinetic equations of Arrhenius and Coats–Redfern with the combustion kinetic parameters of the sludge and rice husk mixture [5]. In this study, the thermogravimetric (TG) and derivative thermogravimetric (DTG) curves are piecewise fitted according to the kinetic model of the co-combustion stage of sludge and rice husk [6]. The co-combustion kinetics of sludge and rice husk is analyzed to provide the theoretical basis for the industrial application of biomass mixed with sludge for combustion and power generation.

2. Materials and methods

2.1. Test materials

The sludge used in the test was taken from a sewage treatment plant in Hubei, Wuhan. The sludge was treated immediately after being recovered from the sewage treatment unit to avoid excessive chemical conversion due to long-term storage of sludge. The rice husk used in the test was taken from the suburbs of Wuhan. The rice husk was milled with a rice mill before the test and baked in oven for 3 h at 105°C. Finally, the rice husk was stored in a desiccator. The industrial analysis of rice husk and sludge referred to the China National Standard [7,8]. Elemental analysis of rice husk and sludge was conducted using an elemental analyzer (German Elementar, Vario EL Cube Element Analyzer). According to the China National Standard [9], the calorific value was determined using the dual-use SDC5015 high-precision automatic calorimeter (Hunan Sande Polytron Technologies Inc.). The results are shown in Table 1.

2.2. Test methods

The rice husk was mixed with sludge at a certain proportion to obtain solid fuel. The mixing ratio is shown in Table 2. The thermogravimetric and microthermogravimetric values of solid fuels were measured by the STA449c/3G thermal analyzer (NETZSCH, Germany). The TG and DTG curves were drawn, and the phase transition law of solid fuels was analyzed. The heating rate was controlled at 20 K/min, the experimental atmosphere was simulated air with the oxygen-to-nitrogen volume ratio of 2:8, and the total gas flow rate was 50 mL/min.

Table.1
Industrial analysis and elemental analysis of raw materials

Sample	Sludge	Rice husk
M_{ad}%	4.5	4.7
A_{ad}%	64.5	4.88
V_{ad}%	25	80.12
FC_{ad}%	6	10.3
C%	14.89	40.72
H%	2.38	5.60
S%	0.67	0.11
N%	2.24	0.26
O%	16.67	39.74
LHV_{ad} (kJ/kg)	6,028	16,010

3. Results and discussion

3.1. Hot and micro-hot weight

The thermogravimetric curve of the combustion of the mixed sample is shown in Fig. 1, and the percentage of mass loss is shown in Table 3. The mass loss of the co-fired samples was mainly distributed among three temperature stages. The first stage occurred at less than 200°C, and the mass loss was less than 6%. When the temperature increased to 200°C, the second stage of mass loss appeared on the thermogravimetric curve. At this stage, the mass loss was obvious, and the thermogravimetric curve decreased sharply. Between 200°C and 400°C, the mass loss accounted for 49.85% to 72.36% of the total weight loss. With increasing rice husk content, the proportion of mass loss also relatively increased.

The mass loss in the third stage occurred between 400°C and 700°C. At this time, the mass loss rate of the sample was in the range 12.174%–25.467%. Compared with the loss rate decrease in the previous stage, the curve was slightly flat. When the temperature was greater than 700°C, the mass tended to be constant, and the loss was less than 1%.

Table 2
Mixed fuel sample

Number	Mixed fuel composition
RH	Rice husk
RS1	10%Dry sludge + 90% rice husk
RS2	20% Dry sludge + 80% rice husk
RS3	30% Dry sludge + 70% rice husk
RS5	50% Dry sludge + 50% rice husk
RS7	70% Dry sludge + 30% rice husk
SS	Sludge

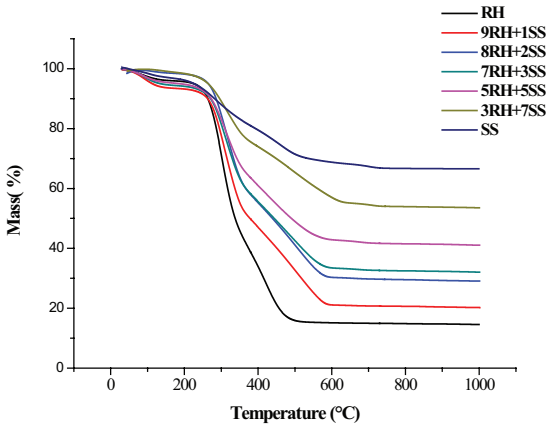

Fig. 1. TG curves of the samples.

Table 3
Mass loss percentage (%)

Sample	<200°C	200°C–400°C	400°C–700°C	>700°C	Mass loss
RH	4.332	61.831	18.859	0.423	85.445
RS1	6.787	46.172	26.264	0.546	79.769
RS2	1.795	42.957	25.467	0.707	70.926
RS3	5.877	38.513	22.880	0.677	67.946
RS5	5.216	33.810	19.155	0.774	58.954
RS7	1.615	24.452	19.381	0.992	46.440
SS	3.822	16.660	12.174	0.766	33.422

In the early stage of the reaction, the weight loss rate of the samples initially increased and subsequently decreased. This finding showed that, when the proportion of sludge was less than 30%, the addition of sludge was beneficial to the combustion of mixed fuel. As the mass ratio of sludge to rice husk increased, the quality of the combustion residue increased significantly. According to the industrial analysis of the raw materials, the ash content of sludge was larger than that of rice husk. Moreover, the output of co-combustion ash increased with the increase in the proportion of sludge.

The thermogravimetric curves of the mixed sample are shown in Fig. 2. As shown in Fig. 2, the two main peaks of the mass loss of rice husk combustion were 44.99% and 36.91%. Comparatively, the three weightless peaks of pure sludge combustion were 15.91%, 12.57%, and 1.56%.

The combustion process of the mixed fuel samples had similar characteristics, and their DTG curves mainly had three weightlessness peaks. The similar characteristics indicated that the combustion kinetics of the mixed fuel samples were similar. This finding showed that the co-combustion process of sludge and rice husk was a multistep reaction process [10]. Related studies showed that the early reaction of the samples was the dehydration process under heating; the reaction at this stage (the first peak) was not discussed [11]. In the middle and late stages of the reaction, combined with industrial analysis, the second peak of the samples was mainly the decomposition and combustion of easy volatile components (light component volatiles) in the raw materials. The third peak was mainly the decomposition and combustion of difficult volatile components (volatile compounds and fixed carbon in macromolecules).

On the basis of the relevant reports in the literature, the sample was mainly in the fat decomposition stage at less than 420°C, whereas the sample was mainly in the protein and carbohydrate decomposition stage at greater than 420°C [12]. In addition, a weightless peak appeared at approximately 650°C during the combustion process of sewage sludge, which can be attributed to a small amount of fixed carbon decomposition in the sludge. The combustion process of sludge and rice husk exhibited the combustion characteristics of the individual combustion of sludge and the combustion characteristics of the individual combustion of rice husk. The co-combustion process could be divided into two stages, that is, (1) easy volatile (light component volatile) precipitation and combustion stage and (2) difficult volatile (volatile compounds and fixed carbon in macromolecules) precipitation and combustion stage [13].

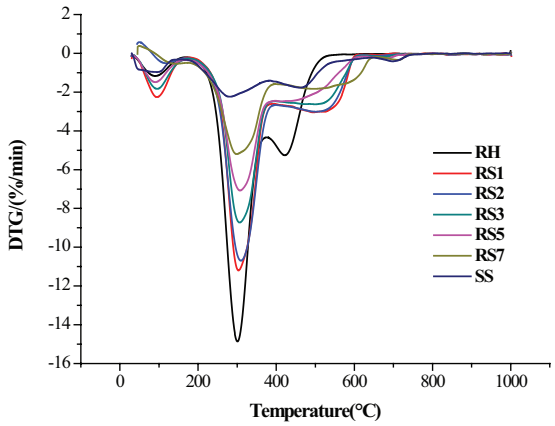

Fig. 2. DTG curve of samples.

The height and width of the combustion peak of the DTG curve could directly reflect the difference of the combustion performance of different samples. The intensity of sample combustion was reflected by the width of the combustion peak. Therefore, the sample reaction performance, ash and combustible components, and other information could be adequately reflected by the DTG curve. Moreover, the performance of ignition, combustion, and burnout of the sample could be comprehensively illustrated by the DTG curve. As shown in Fig. 2, compared with the rice husk curve, the exothermic peaks of the DTG curve from RH1 to RH7 were delayed. This finding showed that the incorporation of sludge inhibited the release of combustible components.

3.2. Kinetic model

The kinetic process of the combustion reaction can be described by the following simple heterogeneous reaction equation:

$$A(\mathrm{S}) \rightarrow B(\mathrm{S}) + C(\mathrm{g}) \quad (1)$$

In this study, the kinetic analysis method of the isothermal homogeneous reaction was used to analyze the heterogeneous reaction at constant heating rate under non-isothermal conditions. The conversion rate was used instead of the concentration parameter in the homogeneous reaction. According to the law of mass action, the reaction rate could be expressed as follows:

$$\frac{d\alpha}{dt} = kf(\alpha) \tag{2}$$

In the formula, α is the fraction of substance A that has already reacted:

$$\alpha = \frac{m_0 - m_T}{m_0 - m_\infty} \tag{3}$$

In the formula, m_0, m_T, and m_∞ denote the sample quality at the beginning of the reaction, sample quality at reaction temperature T, and sample quality at the end of the reaction, respectively, and α denotes the differential reaction mechanism function. The relationship between k and reaction temperature T can be expressed by the following Arrhenius equation:

$$k = A\exp(-\frac{E}{RT}) \tag{4}$$

In the formula, A is the frequency factor, E is the reaction activation energy, and R = 8.314 J/(mol·K) is the gas constant. In this study, the constant heating rate was defined as β:

$$\beta = \frac{dT}{dt} \tag{5}$$

$$\frac{d\alpha}{dT} = \frac{1}{\beta} f(\alpha) A\exp(-\frac{E}{RT}) \tag{6}$$

The mechanism function of the reaction kinetics model was mainly based on the physical and chemical mechanisms of the pyrolysis or combustion reaction. From the point of view of mathematical treatment, the methods used to solve the kinetic parameters mainly include two methods, that is, differential and integral methods. The integral method directly uses the thermogravimetric curve, and the calculation is simple and accurate [14], as follows:

$$G(\alpha) = kt \tag{7}$$

The relationship between differential and integral forms of the dynamic mechanism function satisfies the following relationship:

$$f(\alpha) = \frac{1}{G'(\alpha)} \tag{8}$$

The Coats–Redfern approximation is used in combustion dynamics research [15–17], and the fitting was made by assuming different reaction mechanisms.

Integrating both sides of Eq. (6), the following equation can be obtained:

$$\ln[\frac{G(\alpha)}{T^2}] = \ln\left[\frac{AR}{\beta E}\left(1 - \frac{2RT}{E}\right)\right] - \frac{E}{RT} \tag{9}$$

Given that the value of E for most combustion reactions is $2RT/E \ll 1$, the first item on the right, that is, $\ln\left[\frac{AR}{\beta E}\left(1 - \frac{2RT}{E}\right)\right]$, of Eq. (9) could be approximately regarded as $\ln(\frac{AR}{\beta E})$. Taking $X = \frac{1}{T}$, $Y = \ln\frac{G(\alpha)}{T^2}$, $a = \ln(\frac{AR}{\beta E})$, and $b = -\frac{E}{R}$, the upper form was reduced to $Y = a + bX$. For the appropriate reaction mechanism function $G(\alpha)$, Y and X were linear.

Generally, different reaction mechanisms were observed on both sides of the DTG curve peak. Thus, different dynamic mechanism models were fitted before and after the weightlessness peak of each DTG curve until the maximum correlation coefficient was obtained [18]. The reaction mechanism function was determined, and the activation energy E and the pre-exponential factor A were calculated. The common dynamic reaction mechanism function is shown in Table 4.

Table 4
Commonly used kinetic mechanism functions

Reaction mechanism form	Symbol	$f(\alpha)$	$G(\alpha)$
Phase interface reaction, cylindrical symmetry, n = 1/2	R2	$(1-\alpha)^{1/2}$	$1-(1-\alpha)^{1/2}$
Phase interface reaction, spherical symmetry, n = 1/3	R3	$(1-\alpha)^{2/3}$	$1-(1-\alpha)^{1/3}$
Randomly nucleating and nucleus growth, n = 1	F1	$1-\alpha$	$-\ln(1-\alpha)$
Chemical reaction (grade 2)	F2	$(1-\alpha)^2$	$(1-\alpha)^{-1}-1$
Chemical reaction (grade 3)	F3	$1/2*(1-\alpha)^3$	$(1-\alpha)^{-2}$
One-dimensional diffusion	D1	$1/2*\alpha^{-1}$	α^2
Two-dimensional diffusion	D2	$[-\ln(1-\alpha)]^{-1}$	$\alpha+(1-\alpha)\ln(1-\alpha)$
Three-dimensional diffusion, spherical symmetry, n = 2	D3	$3/2*(1-\alpha)^{2/3}[1-(1-\alpha)^{1/3}]^{-1}$	$[1-(1-\alpha)^{1/3}]^2$
Three-dimensional diffusion, cylindrical symmetry	D4	$3/2*[(1-\alpha)^{-1/3}-1]^{-1}$	$1-2/3*\alpha-(1-\alpha)^{2/3}$
Randomly nucleating and nucleus growth, n = 1/2	A2	$2(1-\alpha)[-\ln(1-\alpha)]^{1/2}$	$[-\ln(1-\alpha)]^{1/2}$
Randomly nucleating and nucleus growth, n = 1/3	A3	$3(1-\alpha)[-\ln(1-\alpha)]^{2/3}$	$[-\ln(1-\alpha)]^{1/3}$
Randomly nucleating and nucleus growth, n = 1/4	A4	$4(1-\alpha)[-\ln(1-\alpha)]^{3/4}$	$[-\ln(1-\alpha)]^{1/4}$

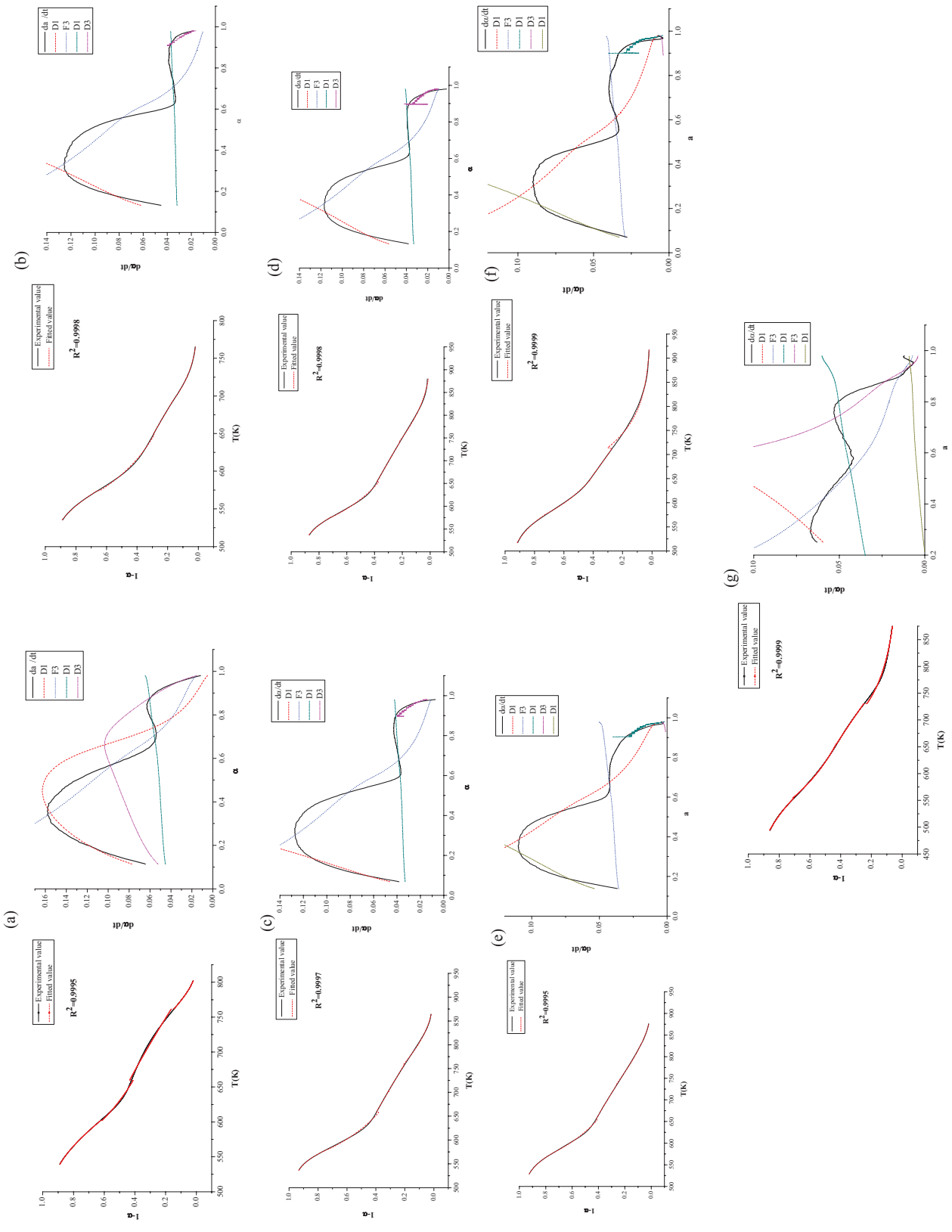

Fig. 3. Comparison between simulated values and actual values of kinetic models (the piecewise fitted graph was on the left and the rate fit graph was on the right): (a) RH, (b) RS1, (c) RS2, (d) RS3, (e) RS5, (f) RS7, and (g) SS.

3.3. Dynamic analysis

The co-combustion of sludge and rice husk was mainly divided into four stages, and some differences in the dynamic parameters were observed at different temperatures. The dynamic parameters of the four stages are analyzed in this study. The results of the piecewise fitting of the TG and DTG curves are shown in Fig. 3.

As shown in Fig. 3 and Table 5, the combustion process of the rice husk sample could be divided into four stages, that is, chemical reaction control stage, chemical reaction control stage, diffusion process control stage, and growth process control stage after random nucleation [19]. The four stages were controlled by different dynamic mechanisms. The combustion process of the sewage sludge sample could be divided into five stages, that is, diffusion process control stage, chemical reaction control stage, diffusion process control stage, chemical reaction control stage, and diffusion process control phase. However, the co-combustion of sludge and rice husk showed different kinetic processes. When the amount of sludge was less than 50%, the combustion process could be divided into four stages. When the amount of sludge was more than 50%, the combustion characteristics of mixed fuel tend to individual combustion characteristics of sludge, and the combustion process could be divided into five stages. The phase transformation of ash at high temperature was not considered in this study. Therefore, the dynamic control mechanism of the first four stages of the co-combustion of mixed fuel was consistent. The first stage was controlled by the diffusion process, the second stage was controlled by the chemical reaction, the third stage was controlled by the one-dimensional diffusion process, and the fourth stage was controlled by the three-dimensional diffusion process (i.e., D1 → F3 → D1 → D3).

Table 5 shows that the activation energy of the late combustion stage of the mixed fuel samples was lower than that

Table 5
Segmentation kinetic parameter of mixed burning of sludge and rice husk

Sample	Temperature range of weightlessness (°C)	Activation energy (kJ/mol)	Frequency factor (s^{-1})	Correlation coefficient	Control mechanism
RH	262–301	84,761	1.63E+07	0.9999	F2
	301–375	56,997	153,313	0.9949	F3
	375–421	17,006	1.131	0.9992	D1
	421–492	37,375	219	0.9985	F1
RS1	266–302	108,331	4.53E+08	0.9974	D1
	302–383	44,250	6,860	0.9846	F3
	383–503	8,576	0.093	0.998	D1
	503–580	50,608	108	0.993	D3
RS2	264–308	155,430	7.76E+12	0.9992	D1
	308–385	43,020	4,286	0.9874	F3
	385–484	11,446	0.187	0.9995	D1
	484–591	11,153	0.152	0.9965	D3
RS3	264–303	97,698	4.15E+07	0.9957	D1
	303–380	42,481	4,349	0.9922	F3
	380–469	10,274	0.146	1	D1
	469–607	38,419	13.288	0.992	D3
RS5	259–305	86,449	3.87E+06	0.9963	D1
	305–372	42,327	4,282	0.9972	F3
	372–433	13,035	0.407	0.9996	D1
	433–606	29,134	2.577	0.987	D3
	606–667	12,899	0.006	1	D1
RS7	243–296	98,887	4.02E+07	0.9985	D1
	296–395	27,488	110	0.9915	F3
	395–492	12,469	0.192	0.9985	D1
	492–659	36,948	6.197	0.9908	D3
	659–704	11,699	0.007	0.9993	D1
SS	221–281	51,006	1,238	0.9982	D2
	281–382	20,250	25.337	0.9978	F3
	382–457	17,091	0.723	0.9985	D1
	457–636	81,195	4.44E+06	0.9913	F3
	636–705	8,773	6.21E+10	0.9924	D1

of the early combustion stage. This finding indicated that the late combustion stage was more difficult than the early combustion stage because the content of volatile matter in rice husk and sludge was higher than that of fixed carbon. The proportion of sludge had a significant influence on the co-combustion process. With the increase in sludge addition ratio, the activation energy initially increased and subsequently decreased. This finding indicated that the combustion process of volatile matter and coke was inhibited by the increase in sludge content. For the different stages of the activation energy of the reaction, in the precipitation stage of the main volatile matter (before and after the first peak), with the increase in heating rate, the activation energy of the reaction decreased. This finding indicated that increasing the heating rate is beneficial to the precipitation of volatile matter. Meanwhile, the second peak indicated that the activation energy of the combustion reaction increased with the increase in heating rate at high temperature. The results showed that the combustion rate of fixed carbon was low and the mass loss was not obvious, such that it should be stimulated and maintained by a high reaction temperature [20].

4. Conclusion

On the basis of the laboratory experiments and data analysis, the following conclusions were drawn:

(1) At temperatures less than 200°C, the first stage of mass loss occurred because of water loss. At temperatures between 200°C and 400°C, the mass loss accounted for 49.85% to 72.36% of the total weight loss because of the decomposition and combustion of easy volatile components. At temperatures between 400°C and 700°C, the mass loss accounted for 22.07% to 41.73% of the total weight loss because of the decomposition and combustion of less volatile components. Moreover, when the proportion of sludge was less than 30%, the addition of sludge was beneficial to the combustion of mixed fuel.
(2) The reaction kinetics mechanisms of sludge and rice husk samples were divided into four stages, that is, diffusion process, chemical reaction process, three-dimensional diffusion process, and one-dimensional diffusion process. The reaction mechanism of volatile matter and fixed carbon in the combustion process is D1 → F3 → D1 → D3.
(3) The activation energy of the late combustion stage of mixed fuel samples was lower than that of the early combustion stage. This finding indicated that the late combustion stage was more difficult than the early combustion stage. With the increase in sludge addition ratio, the activation energy initially increased and subsequently decreased. This finding indicated that the increase in sludge content inhibits the combustion process of volatile matter and coke.

Acknowledgements

The authors acknowledge the technical innovation project of Hubei Province (2016ACA162), the National Key Research and Development Program of China (2017YFC0703300).

References

[1] M.C. Samolada, A.A. Zabaniotou, Comparative assessment of municipal sewage sludge incineration, gasification and pyrolysis for a sustainable sludge-to-energy management in Greece, Waste Manage., 34 (2014) 411–420.
[2] C.S. Xu, A.H. Zhong, X.L. Li, C.M. Wang, A. Sahu, H.M. Xu, T. Lattimore, K.Q. Zhou, Y.Q. Huang, Laminar burning characteristics of upgraded biomass pyrolysis fuel derived from rice husk at elevated pressures and temperatures, Fuel, 210 (2017) 249–261.
[3] M.H. Lopes, P. Abelha , N. Lapa, J.S. Oliveira, I. Cabrita, I. Gulyurtlu, The behaviour of ashes and heavy metals during the co-combustion of sewage sludges in a fluidised bed, Waste Manage., 23 (2003) 859–870.
[4] E.M.M. Ewais, R.M. Elsaadany, A.A. Ahemd, N.H. Shalaby, B.E.H. Al-Anadouli, Insulating refractory bricks from water treatment sludge and rice husk ash, Refract, Ind. Ceram., 4 (2017) 1–9.
[5] M. Otero, L.F. Calvo, M.V. Gil, A.I. Garcia, A. Moran, Co-combustion of different sewage sludge and coal: a non-isothermal thermogravimetric kinetic analysis, Bioresour. Technol., 99 (2008) 6311–6319.
[6] H. Siyuan, J.J. Sheng, An innovative method to build a comprehensive kinetic model for air injection using TGA/DSC experiments, Fuel, 210 (2017) 98–106.
[7] Solid Biomass Fuel Industrial Analysis Method, GB/T 28731-2010, PR China.
[8] Industrial Analysis of Coal, GB/T 212-2008, PR China.
[9] Oxygen Bomb Combustion Method, GB/T 213-2008, PR China.
[10] H. Yilmaz, O. Cam, I. Yilmaz, Effect of micro combustor geometry on combustion and emission behavior of premixed hydrogen/air flames, Energy, 135 (2017) 585–597.
[11] R. Bilbao, J.F. Mastral, M.E. Aldea, J. Ceamanos, M. Betran, J.A. Lana, Experimental and theoretical study of the ignition and smoldering of wood including convective effects, Combust. Flame, 126 (2001) 1363–1372.
[12] H. Zhang, L.L. Zhang, Y.J. Han, Y. Yu, M.A. Xu, X.P. Zhang, L. Huang, S.J. Dong, RGO/Au NPs/N-doped CNTs supported on nickel foam as an anode for enzymatic biofuel cells, Biosens. Bioelectron., 97 (2017) 34–40.
[13] L. Yanfen, X. Ma, Thermogravimetric analysis of the co-combustion of coal and paper mill sludge, Appl. Energy, 87 (2010) 3526–3532.
[14] B.B. Uzun, E. Yaman, Pyrolysis kinetics of walnut shell and waste polyolefins using thermogravimetric analysis, J. Energy Inst., 90 (2016) 825–837.
[15] T. Damartzis, D. Vamvuka, S. Sfakiltakis, A. Zabaniotou, Thermal degradation studies and kinetic modeling of cardoon (*Cynara cardunculus*) pyrolysis using thermogravimetric analysis (TGA), Bioresour. Technol., 102 (2011) 6230–6238.
[16] K.M. Lu, W.J. Lee, W.H. Chen, T.C. Lin, Thermogravimetric analysis and kinetics of co-pyrolysis of raw/torrefied wood and coal blends, Appl. Energy, 105 (2013) 57–65.
[17] H.H. Sait, A. Hussain, A.A. Salema, F.N. Ani, Pyrolysis and combustion kinetics of date palm biomass using thermogravimetric analysis, Bioresour. Technol., 118 (2012) 382–389.
[18] S.V. Vassilev, D. Baxter, C.G. Vassileva, An overview of the behaviour of biomass during combustion: part I. Phase-mineral transformations of organic and inorganic matter, Fuel, 112 (2013) 391–449.
[19] A.B. Folgueras, R.M. Diaz, J. Xiberta, I. Prieto, Thermogravimetric analysis of the co-combustion of coal and sewage sludge, Fuel, 82 (2003) 2051–2055.
[20] S.J. Li, H.L. Wang, J.M. Yan, Q. Jiang, Oleylamine-stabilized Cu0.9Ni0.1 nanoparticles as efficient catalyst for ammonia borane dehydrogenation, Int. J. Hydrogen Energy, 42 (2017) 25251–25257.